WPMST1-CPR(17) 16994

E Lazzaro et al.

Physics conditions for robust control of tearing modes in a rotating tokamak plasma

Preprint of Paper to be submitted for publication in Proceeding of 44th European Physical Society Conference on Plasma Physics (EPS)

This work has been carried out within the framework of the EUROfusion Consortium and has received funding from the Euratom research and training programme 2014-2018 under grant agreement No 633053. The views and opinions expressed herein do not necessarily reflect those of the European Commission.

Physics conditions for robust control of tearing modes in a rotating tokamak plasma

E. Lazzaro[1], D. Borgogno[3], D. Brunetti[1], L. Comisso[4], O. Fevrier[5], D. Grasso[2,3], H. Lutjens[7], P. Maget[6], S. Nowak[1], O. Sauter[5], C. Sozzi[1] and the EUROfusion MST1 Team [a]

[1] *Istituto di Fisica del Plasma - CNR Via R.Cozzi 53, 20125, Milano, Italy*

[2] *Istituto dei Sistemi Complessi - CNR Via dei Taurini 19, 00185, Roma, Italy*

[3] *Dipartimento Energia, Politecnico di Torino Corso Duca degli Abruzzi 24, 10129, Torino, Italy*

[4] *Department of Astrophysical Sciences and Princeton Plasma Physics Laboratory, Princeton University, Princeton, New Jersey 08544, USA*

[5] *Ecole Polytechnique Federale de Lausanne (EPFL), Swiss Plasma Center (SPC), 1015 Lausanne, Switzerland* [6] *CEA, IRFM, F-13108 Saint Paul-lez-Durance, France.,*

[7] *Centre de Physique Theorique, Ecole Polytechnique,CNRS, France.*

[a] *See the author list of Overview of progress in European Medium Sized Tokamaks towards an integrated plasma-edge/wall solution by H. Meyer et al., to be published in Nuclear Fusion Special issue: overview and summary reports from the 26th Fusion Energy Conference (Kyoto, Japan, 17-22 October 2016)

I. ABSTRACT

The disruptive collapse of the current sustained equilibrium of a tokamak is perhaps the single most serious obstacle on the path toward controlled thermonuclear fusion. The current disruption is generally too fast to be identified early enough and tamed efficiently, and may be associated to a variety of initial perturbing events. However a common feature of all disruptive events is that they proceed through the onset of MHD instabilities, and field reconnection processes developing magnetic islands which eventually destroy the magnetic configuration. Therefore the avoidance and control of magnetic reconnection instabilities is of foremost importance and great attention is focussed on the promising stabilization techniques based on localized rf power absorption and current drive. Here a short review is proposed of key aspects of high power rf control schemes (and specifically Electron Cyclotron Heating and Current Drive ECH/ECCD) for tearing modes, considering also some effects of plasma rotation. From first principles physics considerations, here new conditions are presented and discussed to achieve control of the tearing perturbations by means of high power ($P_{EC} \sim P_{ohm}$), in regimes where strong nonlinear instabilities may be driven, such as secondary island structures, which can blur the detection and limit the control of the instabilities. Here we consider recent work which has shown ways of improvement of on some traditional control strategies, namely the feedback schemes based on strict phase tracking of the propagating magnetic islands.

II. INTRODUCTION

The tearing modes have been the subject of extensive studies for many years [1–5]. The first basic linear and nonlinear theory has been subsequently extended to neoclassical regimes [6–8], with bootstrap current effects. Recently the physics understanding has been enriched by new findings on nonuniformity effects on finite magnetic islands, of pressure and temperature associated with energy input [ECRH] and loss (e.g. by radiation) [9–12], rotation and viscosity [16–20, 22], as well as by findings on small scale topological effects of the reconnection [23, 24]. The mutual interaction of tearing modes with shielding effects and coupling and the symmetry breaking effects on global and local plasma rotation have gained great attention, for their important consequences. One of the most promising methods of

controlling magnetic islands is based on driving directly into the magnetic island a current, by absorption of rf waves mainly at the electron cyclotron frequency (ECCD) [26, 27], with a (m, n) helical component counteracting the destabilizing current perturbations. Successful ECCD experiments of NTM control, with different methods, have been carried out in ASDEX Upgrade [28, 29], JT60U [30], FTU [31], DIII-D [32, 33], KStar [34],TCV[35] and EAST [36], and comprehensively reviewed in [37, 38] In a tokamak the task of possible prevention, or effective control of low (m,n) order magnetic reconnection instabilities can rely on few knobs which can be associated just with a few state variables, in a coarse grained picture of the processes. Progress in the physics understanding of the local and averaged effects of rf power absorption is needed to identify the most important limits and bounds; then within these limits one can conceive and design (with state of the art engineering) control systems as insensitive to disturbances as possible (robust), but still responding to the physics to be controlled. The realization of a reliable control scheme based on the steered launch and absorption of high rf power in very precise positions in the tokamak plasma, requires numerous diagnostics and control concepts for robust real time (r-t) operation. The technical implementation of such systems leads to very complex architecture, and this motivates a careful revisitation of the underlying principles to achieve efficiency and reliability. The actual design is the task of professional control engineers, but the formulation of the problem requires the work of expert physicists, capable of isolating the dominant and subsidiary processes, specifying the relevant parameter space, the state and control variables and the eventual acceptable structure of a simplified plant description. The basic tasks for the prevention or control of collapsing events, requires successful means of detection of the unstable modes, in spectrum, amplitude, phase and frequency as well as in choice of strategies of constraint. For instance the generic (albeit formidable) goal of stability must be substantiated in defining the actual desired range of variation of the (main) state variable (e.g. magnetic island width), and the restriction due to subsidiary (unwanted) processes. In this respect it should be borne in mind that the application of intense external coercive means (e.g. boundary magnetic perturbations or ECCD) may lead to violation of the constant ψ regime, on which the governing equation for island evolution is based [1–4]; entering a non constant ψ regime implies the possibility of *driving* instabilities growing faster than the current diffusion process out of the reconnecting region, splitting the fragile X-points into two Y-points and forming secondary islands which blur the identification of the *phase*.

This leads to expect a limit on the amplitude and localization of the externally applied perturbation. The occurrence of multiscale effects (in space and time), as discussed in [48, 49], on one hand, increases the difficulties of selecting control strategies, while, on the other, it offers several possibilities of diagnosing the unstable state. Furthermore in realistic tokamak regimes, account should be taken of plasma toroidal rotation, intrinsic or driven, which alters the stability picture.

III. EQUATIONS FOR RESISTIVE MAGNETIC PERTURBATIONS

For the purpose of this work it is suitable to employ the following incompressible MHD equations

$$\varrho\left[\partial_t \boldsymbol{v} + \boldsymbol{v}\cdot\boldsymbol{\nabla}\boldsymbol{v}\right] = -\boldsymbol{\nabla}p + \boldsymbol{J}\times\boldsymbol{B} \tag{1}$$

$$\partial_t \boldsymbol{B} = \boldsymbol{\nabla}\times(\boldsymbol{v}\times\boldsymbol{B}) - \boldsymbol{\nabla}\times(\eta[\boldsymbol{J} - \boldsymbol{J}_{boot} - \boldsymbol{J}_{CD}]) \tag{2}$$

$$\partial_t p + \boldsymbol{v}\cdot\boldsymbol{\nabla}p = 0 \tag{3}$$

where $\boldsymbol{v}$ is the plasma MHD velocity, p the plasma pressure $\boldsymbol{B}$ the magnetic field and ϱ the mass density which is assumed constant both in space and time. In equation (2) the plasma resitivity η is kept constant, while the current density $\boldsymbol{J}$ is defined by $\mu_0\boldsymbol{J} = \boldsymbol{\nabla}\times\boldsymbol{B}$ (hereafter we normalize $\mu_0 = 1$). Note that in (2) we allow for bootstrap and ECCD corrections to the current density representd by $\boldsymbol{J}_{boot}$ and $\boldsymbol{J}_{CD}$ respectively. In addition we consider here also a sheared equilibrium toroidal flow $\boldsymbol{v}_0 = R\Omega(r)\hat{\boldsymbol{z}}$ (R is the major radius and $\hat{\boldsymbol{z}}$ is the unit vector along the longitudinal direction), satisfying $\varrho\left[\boldsymbol{v}_0\cdot\boldsymbol{\nabla}\boldsymbol{v}_0\right] = -\boldsymbol{\nabla}p_0 + \boldsymbol{J}_0\times\boldsymbol{B}_0$. For small non axisymmetric magnetic perturbations, it is convenient to use the non orthogonal curvilinear coordinate system $u^i = (V(\psi), \theta, \zeta)$, whose arbitrary Jacobian $\sqrt{g} = 1/\nabla V\times\nabla\theta\cdot\nabla\zeta$ here is chosen to be unitary, with $B\cdot\nabla\vartheta = \psi^{'}/\sqrt{g}$. The total magnetic field can be represented in the general form:

$$\mathbf{B} = \psi_t^{'}\nabla V\times\nabla\vartheta - \psi^{'}\nabla V\times\nabla\zeta = \psi^{'}\nabla\times(V\nabla\alpha) \tag{4}$$

where $\alpha = q\vartheta - \zeta$ is a Clebsch magnetic field line label, ψ_t and ψ are the toroidal and poloidal magnetic fluxes, such that the ratio $\psi_t^{'}/\psi^{'}$ is constant at a given flux surface. We introduce the safety factor defined as $q = \psi_t^{'}/\psi^{'}$. It is known that magnetic perturbations described by linearizing the above system, in absence of an equilibrium flow and of an

external current source J_{CD}, may grow unstable at rational surfaces $q(r_s) = \frac{m}{n}$, developing magnetic islands. The first question addressed here is on the role that a background sheared flow may have on these linear resistive instabilities. From previous studies [16, 19, 20] a variety of results is available for discussion. Here we want to propose a first principles discussion based on particular, albeit artificial, flow and q profiles, that have the merit of leading to exact solutions. The basic tool is a form of Newcomb's equation obtained in cylindrical approximation from the linearization of eqs.(1)-(3) written in terms of the reduced MHD variable $\psi = -\frac{rB_0k_\parallel}{m}X$, modified by the presence of a rotation with a simple family of profiles for $k_\parallel$ and rotation. The profiles employed in our analysis are the following

$$k_\parallel(r) = \frac{ns}{\lambda}\left[1 - \left(\frac{r}{r_s}\right)^\lambda\right] \tag{5}$$

$$\Omega(r) = \Omega_0\left[1 - \left(\frac{r}{r_s}\right)^\lambda\right] \tag{6}$$

where n is the toroidal mode number, r_s is the resonant point, s denotes the magnetic shear at r_s and the parameter λ labels the profiles determining their steepness [18]. Note that we chose a reference frame which is moving along the longitudinal direction in a such way that the rotation frequency vanishes at r_s (this is allowed within the cylindrical approximation). Exact solutions in terms of hypergeometric functions can be found and an analytic expression of the classical instability index Δ', with sheared flow, is obtained:

$$r_s\Delta' = -(\frac{m^2-\mu^2}{r_s\lambda})\pi cot\left[\pi(m-\mu)/\lambda\right] \tag{7}$$

$$\mu = (m^2 + 2\lambda + \lambda^2[1+\Theta(y)])^{1/2} \tag{8}$$

where $\Theta(y) = \frac{2y^2}{\lambda^2(1-y^2)}$. It is found (see Fig.1) that the key parameter is the ratio $y = \frac{\Omega'/\omega_A}{q'/q}$ of toroidal rotation shear and magnetic shear [18, 19]. For $y \ll 1$ a weak destabilizing effect due to rotation shear is present, and generally the small m tearing modes are unstable ($\Delta' > 0$), while large m's are stable ($\Delta' < 0$). For $y \sim 1$ a window of stability exists for all m. The response of the nonlinear growth rate $d\ln(w)/dt$ of the neoclassical tearing modes (NTM) to rotation shear, reflects the classical behaviour in reducing the unstable w range, but rotation alone does not seem to provide a reliable control knob. These exact results are in agreement with the form of Δ'_0 derived in toroidal geometry using the WKB approximation ($m \gg 1$), see Ref. [20].

IV. ECH AND ECCD EFFECTS IN THE GENERALIZED RUTHERFORD EQUATION (G.R.E.)

The main task of a theoretical study of rf control of tearing instabilities, in the observable Rutherford phase, is the estimate of the necessary driven current, e.g. the rf power necessary to reduce the state variable $w(t)$ and to design real-time strategies for the rf launching for an effective power deposition and possible tracking of the moving island. A basic question for the design of a control concept is the order of the fastest and slowest time scales of the processes to be controlled (fast reconnection, slow nonlinear growth and saturation, island rotation period), and the associated space scales suggesting how sharp the focusing, radial and/or angular, should be. Moreover, in addition to all the physical scale lengths mentioned above, one has to consider also that the rf-driven current forces another typical scale length, the absorption depth δ_{CD}. This length depends on the wave beam launching and propagation conditions and plasma equilibrium quantities, such as density and temperature. The equation for the evolution of magnetic islands with width $w = 4\sqrt{\psi_s L_s/B}$, larger than the tearing layer is known as Rutherford equation [2]. It is obtained from the rate of flux reconnection with suitable averaging of the Faraday-Ohm equation (2) and it has been generalized to include neoclassical effects, plus the effect of the ECH/ECCD and is coupled to equation for the island rotation frequency ω in the lab frame, similarly obtained from the equation 1 (see, e.g., [39–43]). Here it is convenient to present it in a form currently used in modelling [44]:

$$g_1 \frac{\tau_R}{r_s}\frac{dw}{dt} = r_s\Big[\Delta'_0 + \frac{a_{bs}\Delta_{bs_0} w}{w^2+w_d^2} - \frac{a_{GGJ}\Delta_{GGJ_0}}{\sqrt{w^2+0.2w_d^2}} + \frac{a_{pol}\Delta_{pol_0}\rho_{\theta i}^2 w}{w^4+w_d^4}\frac{\bar{\omega}(\bar{\omega}-\omega_{*i})}{\omega_{*e}^2} - \Delta'_{rf} - \Delta'_w\Big] \quad (9)$$

$$I_\phi \frac{d\omega}{dt} = -T_{0em}(\frac{w}{r_s})^4 \frac{(\omega\tau_w)}{1+(\omega\tau_w)^2} - [\omega-\omega_T]\frac{dI_\phi}{dt} - 4\pi^2\varrho\nu\frac{R^3 {r_s}^3 w}{w^2+w_d^2}[\omega-\omega_T] \quad (10)$$

$$\frac{d\varphi}{dt} = \omega \quad (11)$$

Here τ_R, τ_w are the resistive dffusion time scale and the wall constant [44], ν is a viscosity associated with momentum diffusion and $\bar{\omega} = \omega - \omega_E$,where $\omega_E, \omega_{*e,i}$ are the electric EXB drift and diamamagnetic frequencies and $\omega_T = \omega_E + \omega_{*i} + \kappa(ck_\theta T'_i/eB_0)$, with κ a neoclassical coefficient O(1) [39]. In the torque balance equation, $I_\phi = 4\pi^2\varrho R^3 r_s w$ is the moment of

inertia of the rotating island and the constant T_{0em} is the amplitude of the electromagnetic (em) torque . The term Δ'_0 represents the amplitude of the jump of logaritmic derivative of ψ across the $q = m/n$ surface [1–4] and in presence of a background toroidal rotation must embody the physics described in Eq.7. The dimensionless terms $\Delta_{bs_0} = \beta_p\sqrt{\epsilon} \mid L_q/L_p \mid$, $\Delta_{GGJ_0} = \beta_p\epsilon^2{L_q}^2/(r_s \mid L_p \mid)$, $\Delta_{pol_0} = \beta_p(L_q/L_p)^2 g(\epsilon, \nu_{ii})$, represent, respectively, the bootstrap current J_{bs} effect, [6], a toroidicity effect [3], and the third term represents the polarization current due to an effect of ion inertia [8, 9], which is important at the onset of the NTMs. A conventional, accepted evaluation [41] of the other coefficients is $a_{bs} = 2.6$, $a_{GGJ} = 6$. The last term $\Delta'_w = 2k_\theta(r_s/d_w)^2\frac{(\omega\tau_w)^2}{1+(\omega\tau_w)^2}$, with label w for wall, gives a small stabilization due to the induced currents in the first wall [44]. The quantity w_d in the second (bootstrap current) and third [3] terms of the first equation represents a lower limit of the island width related to the finite ratio of heat conductivities field along and across the B field ($\chi_\parallel/\chi_\perp$), and governs the incomplete flattening of the temperature profile within the island separatrix [45, 46]. It is often replaced by the value w_{marg} below which NTMs self extinguish. The portrait of the stability conditions in the neoclassical collisional regimes shown in the phase plane (dw/dt,w) of Fig.1(top), where the nomenclature is indicated and with the region with $dw/dt > 0$ is apparent. A neoclassical tearing mode, at low β_p is linearly and nonlinearly stable, with $\Delta'_0 \leqslant 0$. At higher β_p the neoclassical NTMs are metastable, without an island, until a seed perturbation (presumably of the same helicity) triggers the growth, proportional to β_p [6, 18, 47]. In Fig.1(bottom), the effect is shown of toroidal sheared rotation on the stability domain, discussed in Section III [18].Recent results show that in condition of low magnetic shear in the plasma core, finite pressure gradient effects can excite *infernal modes* which can trigger tearing sidebands [18] through toroidal coupling. The rf power term is given by the sum of contributions describing the helical and axisymmetric current drive, and of localized heating is[12–14] $\Delta'_{rf} = \Delta'_{CD(m,n)} + \Delta'_{CD(0,0)} + \Delta'_{ECH}$. The effect of the rf driven (m, n) helical current in the magnetic island region is conveniently written in terms of I_{CD}, I_p, the total rf and plasma currents, as $\Delta'_{CD(m,n)} = 32\frac{I_{CD}}{I_p}\frac{L_q}{\delta^2_{CD}}\eta_{mn}(\frac{w}{\delta_{CD}})G_{CD}(r_{dep}, \frac{w}{\delta_{CD}})$ [13, 14]. The ECCD efficiency η_{mn} appearing in this term ([14, 40, 43]) is best fitted analytically by $\eta_{mn,CW}\Big(w/\delta_{CD}\Big) = \frac{0.25}{1+(2/3)(w/\delta_{CD})}$ [14] for the constant (CW) rf application and by $\eta_{mn,50\%}\Big(w/\delta_{CD}\Big) = 0.45\tanh[0.4(w/\delta_{CD})](\frac{\delta_{CD}}{w})^2$ for the phased modulation [14]. The function $G_{CD}(r_{dep}, \frac{w}{\delta_{CD}})$ accounts for the radial misalignment effects[13]. The

axisymmetric current contribution is given by $\Delta'_{CD(0,0)} = 4\frac{L_q}{\delta^2_{CD}}\frac{I_{CD}}{I_p}erfc[w/\delta_{CD}]$ [15]. In addition, the local heating effect of the EC waves power absorbed (by the electrons), gives $\Delta'_{ECH} \propto \frac{16L_q\sqrt{\pi}}{\delta^2_{CD}B_p}P_{EC}\eta_H(\frac{w}{\delta_{CD}})$, due to modification of J_{eq} through the resistivity. From the steady state of eq.9 it appears that for locally peaked temperature profiles, the heating helps reducing the saturation width of the island even if it does not suppress it [40].

For ITER-like plasma parameters ($R_0 = 6.3m, a = 2m, B_0 = 5.3T, r_s \sim 1.6m, I_p(r_s) = 11MA, T_e(r_s) = 7keV, n_e(r_s) \sim n_i(r_s) = 9.5 \cdot 10^{19}m^{-3}, \tau_R = 284s, \beta_{pol} = 0.7, w_{sat} = 0.21m, w_d = w_{marg} = 0.03m, J_{CD} = 0.015MA/m^2, \delta_{CD} = 0.04m$), in Fig.2 it is shown that the contribution of the axisymmetric driven current and of the heating part are of the same order of that of the helical current, in balancing the destabilizing bootstrap Δ'_{bs0} [12]. Since these effects are independent of the island phase stringent requirements on phase tracking appear less motivated.

Furthermore, finite magnetic islands are actually asymmetric with respect to the rational q surface, and the asymmetry is equivalent to a current perturbation which can either have stabilizing effects [10, 11] or destabilizing,when associated with thermal losses.A current perturbation due to variations of the local (Spitzer) resistivity, consequent to radiative cooling of the island interior, has been shown to be destabilizing [11] in combination with asymmetry. Replacing the radiative energy losses by EC heating within a band encompassing the reconnection layer seems therefore a reasonable way to counteract these instabilitiies, also by freezing the reconnection process and it combines favorably with the effect of axisymmetric J_{CD} [11, 12], both being phase independent. For a realistic ITER-like scenario, the plot (dw/dt,w) in Fig.3 for different values of injected J_{CD}, shows the comparable contribution of the helical and the axisymmetric terms [12] as well as the modest difference between the case of a CW application and that of a 50% modulation, perfectly phased Fig.4. In the frame of the G.R.E, one key question is whether to apply a prompt intervention to suppress the island of width w as soon as the instability is detected, or apply continuous pre-emptying control of a finite island within chosen bounds [12, 27–29, 37, 43, 47, 57]. Conventionally an estimate of the power P_{CD} required to quench the island growth is obtained by setting to zero the r.h.s of eq.9, assuming that the power is absorbed at the O-point of the rotating island, with perfect phasing, possibly obtained by entraining the modes by external rotating fields, as done in some exploratory experiments[33]. The required power is given by the

expression[44]:

$$P_{ECmin} = (\frac{w_{sat} w}{w^2 + w_{marg}^2} - 1)\frac{a_{bs}}{a_{CD}}\frac{4(1-f)\delta_{CD}}{\sqrt{\pi} w_{sat}}\frac{J_{bs}}{\eta_{CD} J_{CD}} \tag{12}$$

where $f = a_{GGJ}\Delta_{GGJ0}/a_{bs}\Delta_{bs0}$, neglecting the $\Delta_{pol}$and Δ'_w contributions. Many discussions have been made on the advantages of modulating the rf power to deposit the J_{CD} as close as possible to the O-point in synchronism with the island rotation. Actually the parallel transport is virtually instantaneous, such that the driven current density becomes a flux function, on the island flux tubes intercepted anywhere by the rf beam having a deposition spot of finite angular and radial width, and an automatic modulation occurs, encompassing the O-point for a deposition in the range $0 < \alpha < \pi$, if the radial deposition is within $\delta_{CD} \sim w/2$. So the ECCD efficiency varies moderately between a CW and a phase modulated case [54] and what really matters is minimizing the radial mismatch within a range of the order proposed for instance, in Ref.[37]. In the ITER-like case presented, the control of a 2/1 NTM is obtained with a reduction of the EC power $\sim 0.098\%$, about 400 KW. The ECCD (helical) efficiency is illustrated in Fig.5, as function of the ratio w/w_{marg}; considering a radial misalignment $\delta R \sim 0.016m$ from the island O-point, the efficiency is much reduced while $w \leq \delta_{CD} = 0.04m$, recovering for $w > \delta_{CD}$. To illustrate the destabilizing effect of a radial misalignment, which favors the rf power absorbtion across the separatrix, Fevrier et al [50] have proposed a heuristic correction to the efficiency $\eta_{CD} \propto (1 - (\frac{\delta R}{\alpha})^2)\exp[-(\frac{\delta R}{\beta})^2]$, where α, β are profile scale lengths. In conclusion, when the measurements of amplitude ($\propto w^2$), and phase are available with sufficient accuracy, the G.R.E provides a very useful model of the process to be controlled, adopting relatively well established systems [21]. However for the reliability of the control system, with high power circulation, also consideration is needed of possible internal parasitic processes .

V. ECCD MAGNETIC ISLAND SUPRESSION AS CONVERSE OF A FORCED RECONNECTION PROBLEM

In this section the attention is addressed to subtler physical effects which may occur on smaller space scales, albeit in a restricted range of operative parameter. It is convenient to isolate the problem in the frame of a simplified model. The effect of an external current source, parallel to the magnetic field and driven by rf power absorption, namely ECCD, [26]

can be usefuly mocked-up in a plasma slab. Then the effect of ECCD, can be investigated as a converse of the Hahm Kulsrud Taylor (HKT) [52, 53] forced reconnection problem starting from the equilibrium II of [52] which corresponds to a state with a magnetic island.The basic elements a of the classical HKT problem, are used, adopting the notation of Refs.[24, 51] for the reduced MHD description of the magnetic field through a flux function ψ and a velocity stream function ϕ (electrostatic potential). Dimensionless variables are defined and used dropping hats:

$$\hat{x} = x/a, \hat{t} = \tau/\tau_A, \hat{\psi} = \psi/aB_0, \hat{\phi} = \phi/a^2\tau_A, \hat{J}_{CD} = J_{CD}a/B_0, S = \tau_R/\tau_A, \hat{\partial_{xx}}\hat{\phi_1} = \hat{\phi_1^"} \quad (13)$$

In this dimensionless model $\eta = S^{-1}$, the inverse Lundquist number, and $\nu = P\eta$, with P the Prandtl number. In the case of the HKT problem the equilibrium configuration is given by $\psi_0 = -x^2, \phi_0 = 0$. Here the equilibrium is $\psi_{II}(x,y) = \Psi_\Sigma \frac{\cosh(kx)}{\cosh(k)} cos(ky), \phi_0 = 0$, where $\Psi_\Sigma \propto {w_0}^2$ and w_0 is the initial island width. The first order Faraday-Ohm and vorticity equations for the dynamics in the visco-resistive regime [17, 24] of the inner layer, where reconnection occurs, include an external, localized current source :

$$\partial_t \psi_1 + kx\phi_1 = \eta[\psi_1^" - J_0 D(\psi)] \quad (14)$$

$$\partial_t \phi_1^" = kx\psi_1^" + \nu\phi_1^{""} \quad (15)$$

The current distribution $D(\psi)$ on the intercepted flux surfaces can be modeled as a function of ψ, which, without loss of generality can be chosen to be a Gaussian:

$$J_{CD} = \frac{2J_0}{\delta_{CD}\sqrt{\pi}} \exp[-\frac{4(x - x_{dep})^2]}{\delta_{CD}^2}] \quad (16)$$

With a furher change of variable $\hat{x} = kx$ the time-Laplace and space-Fourier transforms of Eqs.(14, 15) are performed, and with tedious but straightforward algebra as in [24] an equation is obtained for the Fourier transform ϕ_F of the electrostatic potential and a consequent expression for the reconnected flux ψ_F. Taking into account that using J_{CD} as a compact distribution, or in the limit case of a Dirac' s delta, the drive term gives a vanishing contribution in the equation for ϕ_F,we obtain:

$$\partial_\theta(\frac{\theta^2}{s + \eta k^2\theta^2}\partial_\theta\phi_F) - (s\theta^2 + \nu k^2\theta^4)\phi_F = 0 \quad (17)$$

and the expression of the Laplace transformed ψ_L on the x=0 layer is:

$$\psi_L(0,s) = \frac{2i\eta k^2}{s}\int_0^\infty d\theta \frac{\theta^2}{s + \eta k^2\theta^2}\partial_\theta\phi_F - \frac{\eta J_0 D(0,s)}{s} \quad (18)$$

The boundary conditions to be applied to Eq.(15,17) are $\lim_{\theta\to\infty}\phi_F(\theta,s)=0$. In the visco-resistive range $s \ll \eta k^2\theta^2$ the asymptotic matching of the small and large inner solutions with the outer (ideal) solution, and application of boundary conditions, results in:

$$\Psi_L(0,s)=\psi_{out}(0,s)=\frac{\Delta'_s\Psi_\Sigma}{(\Delta'(s)-\Delta'_0)s} \tag{19}$$

where $\Delta'_0=-\frac{2k}{\tanh k}$ and $\Delta'_s=\frac{2k}{\sinh k}$ and $\Delta'(s)=s\tau_{\nu\eta}$ results from the matching of the solutions in the overlapping interval and $\tau_{\nu\eta}\propto\nu^{1/6}\eta^{-5/6}k^{-1/3}$. The boundary value which in Hahm Kulsrud is a driving term, here corresponds to the flux label of the separatrix, proportional to the square of the initial magnetic island. At this point, following the procedure of Ref.[24], we just replace $\Psi_L(0,s)$ with $\Psi_L(0,s)-\frac{\eta J_0}{s}D(0,s)$, obtaining

$$\Psi_{ext}(s)=[\Psi_\Sigma-\frac{(\Delta'(s)-\Delta'_0)}{S\Delta'_s}J_0D(0,s)] \tag{20}$$

It appears from Eq.(20) that a good choice of $J_0(t)$ can control the reconnected flux amplitude, i.e the island width. This condition can be expressed in terms of a partial suppression parameter G, $(0<G<1)$ and eq.20 gives

$$\frac{(\Delta'(s)-\Delta'_0)}{S\Delta'_s}J_0D(0,s)=G\Psi_\Sigma \tag{21}$$

The combination of eq.20 with the solution of eq.15 in the ideal limit (vanishing torque), gives eventually the expression of the converse HKT problem in the $-1<x<1, -\pi<ky<\pi$ slab:

$$\psi(x,s)=\Psi_{ext}(s)[\cosh(kx)-\frac{\sinh|kx|}{\tanh(k)}]cos(ky)+\Psi_\Sigma\frac{\sinh|kx|}{\sinh(k)}cos(ky) \tag{22}$$

Before discussing the final controlled state it should be observed that when the island, in the constant ψ regime, shrinks below a critical value, if the driven current has a scale length (absorption depth) comparable with this critical value, it can drive the perturbation into a non-constant ψ regime, where marginal, nonlinear instability conditions can be reached for tearing unstable current sheets and secondary island structures. Indeed, in the viscoresistive regime, according to[24, 25], a nonlinear instability condition should be reached when, under the ECCD effect, the island approaches from above (in a controlled fashion), the dimensionless critical width $w_{crit}=4\sqrt{\Psi_{crit}}$:

$$\Psi_{ext}=\Psi_{crit}=C\frac{k}{\Delta'_s}\frac{\sqrt{(1+P)}}{S} \tag{23}$$

where C is a parameter related to the marginally stable current sheet aspect ratio. Recalling previous definitions, since here the value Ψ_Σ at the boundary is fixed and k is a parameter to be determined by consistency conditions, the critical condition is transferred to the current peaking ratio J_0/δ_{CD} (here dimensionless):

$$\frac{2J_0}{\delta_{CD}\sqrt{\pi}} \gtrsim \frac{S\Delta'_s}{(\Delta'(s)-\Delta'_0)s}[\Psi_{crit}-\Psi_\Sigma] \tag{24}$$

Using the feedback relation eq.21 and eq.23 condition 24 becomes:

$$\frac{J_0}{\delta_{CD}} \gtrsim \frac{\sqrt{\pi}}{2}\Big(\frac{G}{1+G}\Big)\frac{Ck\sqrt{1+P}}{(-\Delta'_0)} \tag{25}$$

If this ratio is exceeded, the non-constant ψ regime is entered, where the collapse of the X-points and *cariokinesis* into secondary structures is possible. This unstable regime will eventually saturate into a controlled equilibrium condition dominated by the rf driven current. In such condition the constant C can be taken as $C = \frac{2}{\sqrt{\pi}}\Big(\frac{1+G}{G}\Big)\frac{(-\Delta'_0)}{\sqrt{1+P}}\frac{J_0}{m_p}$, where m_p is a small number, so that the wavenumber is $k = m_p/\delta_{CD}$. The topology of the $q = m/n$ rational surface is preserved, if we consider $q = (m+m')/(n+n')$ leading to $k = k_0 + k' \sim m_p k_0$. The above value of C, is compatible with the formation of current sheets of aspect ratio $\epsilon_c > C^{-1/2}$. In the case of small (dimensionless) J_0, the wavenumber k should result from a consistency condition imposed by matching the (transition) from the (constant- ψ) Rutherford regime, characterized by $\Psi_{ext} \sim P^{1/6}S^{-1/3}k^{-1/3}{\Delta'_s}^{-1}$ [24] to the (non-constant- ψ) nonlinear regime characterized by the threshold condition Eq.23. The consistency relation then is $k = P^{1/8}S^{1/2}(1+P)^{-1/2}C^{-3/4}$. The analytic expression (22) plotted in Fig.6 shows in the first frame the intitial ψ_{II} state, with islands, in the second frame the suppressed state with the J_{CD} annihilating Ψ_{ext} and in the third frame the effect of narrowing the J_{CD} profile width by 20% at total constant current, with reappearance of islets and current sheets. This is to be expected since it corresponds to an increase of the peaking current ratio eq.25.

An illuminating similar result has been obtained by carrying on a set of numerical experiments of magnetic island control assuming the Reduced Resistive MHD model in slab geometry, described in ref.[48]. The simulations, performed in the 2D slab geometry, are aimed to control the magnetic island rising from a spontaneous reconnection event in presence of a static, linearly unstable Harry's pinch equilibrium $\phi_{eq} = 0$, $\psi_{eq}(x) = -\log(\cosh(x))$. The current drive is applied continuously starting from a large nonlinear magnetic island. Fig.7 shows the magnetic configuration at the time when the ECCD injection starts (left

frame) and the time evolution of the magnetic island area in absence of control.
Different widths of the ECCD beam deposition have been adopted, while the initially injected total ECCD current, $\int J_{CD}(x, y, t_1)dxdy$, where t_1 is the initial deposition time, is the same. The center of the ECCD beam is constant and located at the O-point of the magnetic island at $t = t_1$. Fig.8 shows, from top to bottom, the effect of the ECCD beam injection for three different values of $\delta_{CD} = b \cdot w(t_1)^2/2$, with $b = 0.5, 1, 2$, where $w(t_1)$ is the magnetic island half width at $t = t_1$. In each row, corresponding to a specific value of b, the left frame shows the plasma current at a fixed time with, superimposed, the magnetic surfaces crossing at the X-points. The right frame shows the evolution of the reconnected area, i.e. the area of the region enclosing magnetic surfaces with a different topology compared to the equilibrium configuration. It reduces to the area of a magnetic island when a single mode dominates over the others.
We observe that in all the cases considered here the system moves towards a stationary configuration where the area of the reconnected region is comparable with the area of the magnetic island at the initial deposition time. However the current control has a significant effect on the change of the magnetic topology compared with the initial magnetic island. Moreover this change appear to be strongly dependent on the value of the beam width. The numerical analysis shows that the new topology is the results of a complex dynamics induced by the continuous deposition of the J_{CD}. After an initial phase when the J_{CD} reduces effectively the magnetic island, in fact, the small scale current layers induced by the external control current along the null axis $x = 0$ give rise to plasmoid like secondary structures. These structures grow and recombine on fast time scales, leading to a continuous change of the magnetic topology untill the saturation is reached. Note that the smaller the b parameter, the more lively the dynamics. Therefore the striking result is that the ECCD current injection, meant to suppress the Rutherford magnetic islands, can lead to formation of a secondary island chain on the scale of δ_{CD}, as shown in Fig.8 In practice,with the broad beam focussing of ITER-like cases similar to the example presented the (dimensionless) peaking parameter $\frac{J_0}{\delta_{CD}} \sim 0.36$ can exceed the critical value only for nearly vanishing local Prandtl number P. Nonlinear formation of secondary islands, expected in systems with large amount of free energy, has not been often documented in tokamak experiments. However interesting observations have been recently reported in JET (without ECH) and COMPASS [55] and in FTU [56] in presence of ECH. In designing control systems based on delivering large rf

power with sharply focussed beams, the associated nonlinearities should be considered.The possible occurrence of such nonlinear substructures, shown in Figs.8, clearly hampers the use of the phase as a measurable and controllable variable.

VI. DETECTION AND CONTROL ISSUES: FEEDBACK AND OPTIMAL CONTROL POLICY

The physical objective is to reduce the island width to zero in minimal time injecting $ECRH/ECCD$ at the position of the q=m/n surface, identified, for instance, by preliminary equilibrium reconstruction and by ECE signals correlation methods, possibly in phase with the Mirnov coils signals, analysed in r-t by a digital PLL (phase-locked loop and Singular Value Decomposition (SVD) methods[56]. The variety of the signals to be acquired and processed for the control action, and their intrinsic uncertainties as well as those of the model predictions could be too high for the feedback specification, while the sensitivity is in principle infinite. The direct measurements are characterized instead by a lower uncertainty but with finite sensitivity due mainly to noise. It can therefore be proposed to use a combination of both using a probabilistic approach based on the Bayesian assimilation in real time of all the information available [56]. An important advantage of using more than one source of information is the possibility to increase the robustness of the estimate by comparing the consistency among the available data. In the well known plot dw/dt vs w of the (nonlinear) growth rate for NTMs (see Figs.(1,3)), the early unstable growth interval before the maximum is where a most effective mode tracking and amplitude control *should* be applied. In this interval the NTM control problem can be cast into a linearized form belonging to a general class known in the theory of multistage decision processes [58]. The governing equation (9) for the (dimensionless) state vector $\boldsymbol{X(t)} = [W/r_s, (\omega - \omega_\star)/\omega_{\star e}]$, with the initial condition $\boldsymbol{X(0)} = \boldsymbol{X_0}$, and a control vector function $\boldsymbol{U(t)}$ can be written as:

$$\frac{d\boldsymbol{X}}{dt} = \boldsymbol{A} \cdot \boldsymbol{X} + \boldsymbol{B} \cdot \boldsymbol{U} + \boldsymbol{n} \tag{26}$$

where the matrix $\boldsymbol{A}$ is obtained from the linearized G.R.E. eqs.(9,10),and $\boldsymbol{B} = [\boldsymbol{b}]$ is the matrix of control coefficients,while $\boldsymbol{n}$ represents a noise input, heretofore neglected. In this

example $\boldsymbol{A}$ has the structure:

$$\boldsymbol{A} = \begin{pmatrix} a_{11} > 0 & a_{12} < 0 \\ a_{21} < 0 & a_{22} < 0 \end{pmatrix} = \begin{pmatrix} O(X_t^{-1}) & O(X_t^{-3}) \\ O(X_t^{2}) & O(X_t^{-2}) \end{pmatrix} \quad (27)$$

where $X_t = w_t/r_s \ll 1$ is the NTM seed threshold island value, above which the mode grows unstable [6]. The formal problem consists in reducing the state $\boldsymbol{X(t)}$ to zero in minimal time by a suitable choice of the control function $\boldsymbol{U(t)}$. The latter, when the actuator is the ECH/ECCD launching system, can be represented in terms of a function of the radial misalignment δR between the wave beam deposition position (minor radius) r_{dep} and the rational q surface $r_{m,n}$ where magnetic islands appear, and of the phase mismatch $\delta\phi$:

$$\boldsymbol{U(t)} = [h \exp(-[r_{dep} - r_{m,n}]^2), \delta\phi] \quad (28)$$

Near the threshold value $X_t \ll 1$ the rank of the system matrix $\boldsymbol{A}$, is full, but the Kalman controllability matrix $\boldsymbol{Q} = [\boldsymbol{b}, \boldsymbol{Ab}]$ is of full rank only if the coefficients a_{21} proportional to perpendicular viscosity and a_{22}, to first wall resistivity are not vanishing. This actually means that the mode rotation and phase is hardly controllable, and therefore a feedback design should probably aim primarily at minimizing the control U which in the equation 27 appears linearly, although dependence on the radial mismatch $\delta R^2 = [r_{dep} - r_{m,n}]^2$ is exponential, mimicking the EC power absorption line.It is then useful to explore an approach of optimal control, complementary to the usual feedback schemes, and based,for instance, on the constrained minimization of a "soft landing" cost function

$$J = \int_0^T dt[U^2 + 1] \quad (29)$$

subject to the fulfilling of Eq.(26). The optimal control approach, by weighting the elements of the model and of the controller,can combine requirements of robustness and response to the physics. The constrained problem is solved introducing the Hamiltonian from which the adjoint problem is formulated

$$H(\boldsymbol{X}, \boldsymbol{p}) = 1 + U^2 + p_1 \frac{dX_1}{dt} + p_2 \frac{dX_2}{dt} \quad (30)$$

$$\frac{dp_1}{dt} = -\frac{\partial H}{\partial X_1}, \frac{dp_2}{dt} = -\frac{\partial H}{\partial X_2}, \frac{\partial H}{\partial U} = 0 \quad (31)$$

For this simple example the instructive solution is analytic:

$$X_1 = X_{01} e^{a_{11}t} + \frac{X_{02} a_{12}}{a_{22} - a_{11}} [e^{a_{22}t} - e^{a_{11}t}] - U(t) \frac{e^{a_{11}t}}{a_{11}} \sinh(a_{11}t) \quad (32)$$

$$X_2 = X_{02}e^{a_{22}t} (33)$$

$$U(t) = \frac{a_{11}e^{-a_{11}t}}{\sinh(a_{11}T)}[X_{01}e^{-a_{11}T} + \frac{X_{02}a_{12}}{a_{22}-a_{11}}[e^{a_{22}T} - e^{a_{11}T}]] \quad (34)$$

The parameters of the exercise are deduced from a real TCV discharge [59].The perturbation of the frequency decays on the timescale $1/a_{22}$. The result in Fig.9 (top) shows that a suitable control of the beam can quench the mode amplitude in the case of fixed radial misalignment $\delta R^2 = const.$ Eq.34 shows that the control amplitude is proportional to the *initial rate of growth* of the magnetic island, with a correction due to the intial mode perturbed rotation, which here is decaying; since the latter is not precisely measurable, the control geared on the measurement of the mode r.m.s growth rate is sufficient to bring the amplitute to target. A feedback system based on phase tracking may loose accuracy when secondary structures appear, blurring the phase detection as shown in Fig.8 [56]. Then it is advantageous to complement such systems with optimal control policies. Since it turns out that what is important is the radial focussing, it is interesting to explore a piecewise optimal policy where the control function $U(t)$ is extended allowing for a time dependence of $|\delta R(t|) = \delta_\epsilon|\Sigma(2\frac{2t}{\tau_\Sigma} - 1))| \sim w$ with $\Sigma(t)$ a triangle waveform representing an intermittent scanning of the neighborhood of the rational surface:

$$U(t) = \frac{a_{11}e^{-a_{11}t}f_\Sigma(t)}{\sinh(a_{11}T)}[X_{01}e^{-a_{11}T} + \frac{X_{02}a_{12}}{a_{22}-a_{11}}[e^{a_{22}T} - e^{a_{11}T}]] \quad (35)$$

The result in Fig.9 (bottom) shows that a suitable intermittent steering of the beam across the rational surface, pre-determinined by equilibrium identification,with $f_\Sigma(t) = \exp(-(\delta R(t)/\alpha)^2)$ can substantially quench the mode amplitude also in the extreme case of missing or ineffective control of the phase, reaching robust performance.

The results of modelling with the extended MHD code XTOR [50], reproduced in Fig.10 are very similar to those of the above model. Some recent successful experiments,shown in Fig.11 [35, 54, 56, 57] have used intermittent beam steering techniques for pre-emptive stabilization of NTM's and can be interpreted with help of the above conceptual model. A practical steering of the rf beam across the target surface could probably be performed more easily using the FADIS wave beams steering system[50, 60]. Another example of NTM amplitude control using a similar method is shown in Fig.12 [56]. Here NTMs are reduced in amplitude with an EC beam scanning the $q = m/n$ surface from the low field side. Also pre-emptying approaches to stability conditions, should be favoured by wave beam space

scales not to close to the critcal value 25. A beam deposition depth $\delta_{CD} \geq w$ is energetically less efficient but safer, and with suitable pacing intermittency, it favors slower processes and keeps conditions of (linear) observability and controllability.

VII. CONCLUSIONS

The growing complexity of the achitecture of detection and control systems for tearing instabilities in tokamaks requires a careful selection of priorities in the objectives and tasks. With actuators delivering large, localized power to the system, feedback techniques may be limited by the possible onset of smaller scale phenomena in a non-constant ψ regime,which may blur detection and hinder the stabilization process. The combination of feedback with optimal control policies, can help obtaining the necessary robust performance.

Acknowledgments. This work has been carried out at the Istituto di Fisica del Plasma CNR, within the framework of the EUROfusion Consortium and has received funding from the Euratom research and training programme 2014-2018 under grant agreement No 633053. The views and opinions expressed herein do not necessarily reflect those of the European Commission.

VIII. REFERENCES

[1] Furth H P, Killeen J and Rosenbluth M N 1963 Phys.Fluids **6** 459

[2] Rutherford P H 1973 Phys. Fluids **16** 1903

[3] Glasser A H, Greene J M and Johnson J L 1975 Phys.Fluids **18** 87588

[4] Ara G, Basu B,Coppi B, Laval G, Rosenbluth M N, and Waddel B V. Annals of Physics 1978 **112** 443

[5] Hastie R J, Sykes A, Turner M and Wesson J A 1977 Nucl.Fusion **17** 515

[6] Callen J D et al, *Proceedings of IAEA Conference Plasma Physics and Controlled Nuclear Fusion Research*1987, Vol 2 (Vienna: IAEA) p.157).

[7] Fitzpatrick R 1988 Phys. Plasmas **5** 3325

[8] Mikhailovskii A B 2003 Contrib. Plasma Phys. **43** 125

[9] Smolyakov A I and Lazzaro E 2004 Phys.Plasmas **11** 4354

[10] Smolyakov A I et al 2013 Phys.Plasmas **20** 062506

[11] White R et al 2015 Phys. Plasmas **22** 022514

[12] Westerhof E et al 2016 Nucl. Fusion **56** 036016

[13] De Lazzari D and Westerhof E 2009 Nucl. Fusion **49** 075002

[14] Sauter O 2004 Phys. Plasmas **11** 4808, 2004.

[15] Bertelli N, De Lazzari D and Westerhof E 2011 Nucl. Fusion **51** 103007

[16] Chen X L and Morrison J P 1990 Phys. Fluids B **2** 495

[17] Fitzpatrick R 1993 Nucl. Fusion **33**1049

[18] Brunetti D, Lazzaro E, Nowak S 2017 Plasma Physics and Controlled Fusion **59** 055012

[19] Chandra D,Sen A,Kaw P et al 2005 Nucl. Fusion **45** 524530

[20] Sen A et al, 2013 Nucl. Fusion **53** 053006

[21] Hennen B A, Westerhof E,Nuij P W J M. et al 2010 Plasma Phys. Control. Fusion, **52** 104006

[22] Mikhailovskii A B, Pustovitov V D and Smolyakov, A I 2000 Plasma Physics and Controlled Fusion**42** 309,

[23] Loureiro N F, Cowley S C, Dorland W D, Haines M G, and Schekochihin A A, 2005 Phys.Rev. Lett.**95** 235 003

[24] Comisso L, Grasso D, and Waelbroeck F L 2015 Phys. Plasmas **22** 042109

[25] Comisso L, Lingam M, Huang Y-M, Bhattacharjee A, 2016 Phys. Plasmas **23** 100702

[26] Fisch N J and Boozer A H 1980 Phys. Rev. Lett. **45** 720

[27] Perkins F W, Harvey R W, Makowski M and Rosenbluth M N, "Prospects for electron cyclotron current drive stabilization of neoclassical tearing modes in ITER," 17th IEEE/NPSS Symposium Fusion Engineering (Cat. No.97CH36131), San Diego, CA, 1997, pp. 749-751 vol.2.

[28] Gantenbein G, Zohm H, Giruzzi G, Gnter S,Leuterer F, Maraschek M, Meskat J, Yu Q, ASDEX Upgrade Team, and ECRH-Group (AUG) 2000 Phys. Rev. Lett. **85** 1242

[29] Zohm H, Gantenbein G, Giruzzi G, Gnter S,Leuterer F, Maraschek M, Meskat J, Peeters A G, Suttrop W, Wagner D, Zabiego M, ASDEX Upgrade Team, and ECRH Group et al 1999 Nucl. Fusion **30** 577

[30] Isayama A, Kamada Y, Ide S, Hamamatsu K, Oikawa T, Suzuki T, Neyatani Y,Ozeki T, Kajiwara K, Ikeda Y, and the JT-60 team 2000 Plasma Phys. Control. Fusion **42** L37

[31] Berrino J, Cirant S, Gandini F, Granucci G, Lazzaro E,Jannone F, Smeulders P, and DAntona G 2006 IEEE Trans. Nucl. Sci. **53** 1009

[32] Petty C C, La Haye R J, Luce T C,Humphreys D A, Hyatt A W,Lohr J, Prater R, Strait E J and Wade M R. 2004 Nucl. Fusion **44** 243

[33] Volpe F A G, Austin M E, La Haye R J, Lohr J, Prater R,Strait E J, and Welander A S 2009 Phys. Plasmas **16** 102502

[34] Seol J C,Lee S G,Park B H , et al 2012 Phys. Rev. Lett **109**, 195003

[35] Felici F, Rossel J X,Canal G, et al 2012 Nucl. Fusion **52** 074001

[36] Wang S, Ma Z W, and Zhang W. 2016 Phys. Plasmas **23** 052503

[37] Pletzer A and Perkins F W 1999 Phys. Plasmas **6** 1589

[38] Prater R, La Haye R J, Lohr J, Luce T C, Petty C C, Ferron J R, Humphreys D A, Strait E J, Perkins F W, and Harvey R W 2003 Nucl. Fusion **43** 1128

[39] Ramponi G, Lazzaro E and Nowak S, 1999 Phys. Plasmas **6** 3561

[40] Hegna C C and Callen J D 1997 Phys. Plasmas **4** 2940

[41] Sauter O et al 1997 Phys. Plasmas **4** 1654

[42] Zohm H 1997 Phys. Plasmas **4** 3432

[43] Giruzzi G, Zabiego M,Gianakon T A, Garbet X, Cardinali A, and Bernabei S 1999 Nucl. Fusion **39** 107

[44] Nowak S, NTM stabilization, 2014 Deliverable F4-D-22P4BW - 01D0201

[45] Fitzpatrick R and Hender T C 1994 Phys. Plasmas **11** 3337

[46] Fitzpatrick R 1995 Phys. Plasmas **2** 825

[47] La Haye R J 2006 Phys. Plasmas **13** :055501

[48] Borgogno D, Comisso L, Lazzaro E, and Grasso D 2014 Phys. Plasmas **21** 060704

[49] Grasso D, Lazzaro E, Borgogno D and Comisso L 2016 Journal of Plasma Physics, **82**(6)

[50] Fevrier O, Maget P, Lutjens H, Beyev P 2017 Plasma Physics and Controlled Fusion **59** 044002

[51] Fitzpatrick R 2003 Phys. Plasmas **10** 2304

[52] Hahm T S and Kulsrud R M 1985 Phys. Fluids **28**, 2412

[53] Lazzaro E and Comisso L 2011 Plasma Physics and Controlled Fusion **53**, 054012

[54] Fevrier O, Maget P, Lutjens, Luciani J F, Decker J, Giruzzi G, Reich M, Beyer P, Lazzaro E, Nowak S, and the ASDEX Upgrade team 2016 Plasma Phys. Control. Fusion **58**, 045015

[55] Salzedas F and JET EFDA Contributors 2011 Phys. Plasmas **18**100701

[56] Sozzi C, Galpert G,Alessi E, et al 2015 Nucl. Fusion **55** 083010

[57] Sauter O, Henderson M A,Ramponi G, Zohm H,Zucca C2010 Plasma Physics and Controlled Fusion **52** , 025002

[58] LaSalle J P Time optimal control systems 1959 Proc. Natl. Acad. Sci. USA **43** , 573577

[59] Lazzaro E,Nowak S,Sauter O et al, 2015 Nucl. Fusion **55**, 093031.

[60] KasparekW, Petelin M, Shchegolkov ., Erckmann V, Plaum B, Bruschi A, at IPP Greifswald, E. G., Karlsruhe, F., and Stuttgart, I. 2008 Nuclear Fusion **48** 054010.

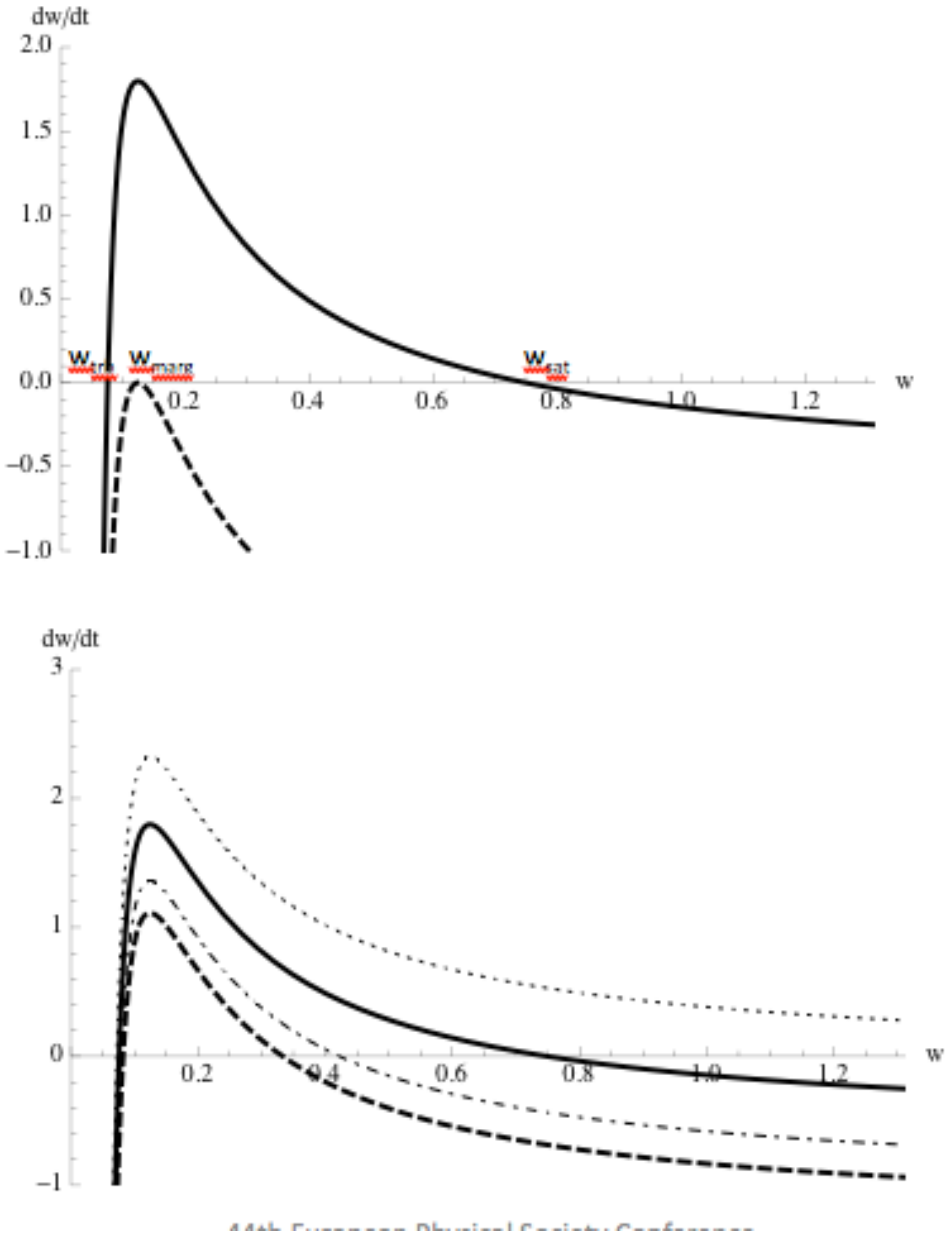

FIG. 1. *(top) Sketch of dimensionless neoclassical growth rate dw/dt vs w (m=2) with indication of nomenclature and of the condition of mode stabilization by EC driven current.;(bottom) Neoclassical growth rate dw/dt v vs w for NTM modes (m=2) parameterised in terms of the ratio y(flow shear/magnetic shear):(dots) y=0.6,(full) y=0,(dotdash) y=1.1, (dash)y=1.4. The shear ratio y hardly affects the threshold and marginal values of the island width while the saturation width may change considerably.*

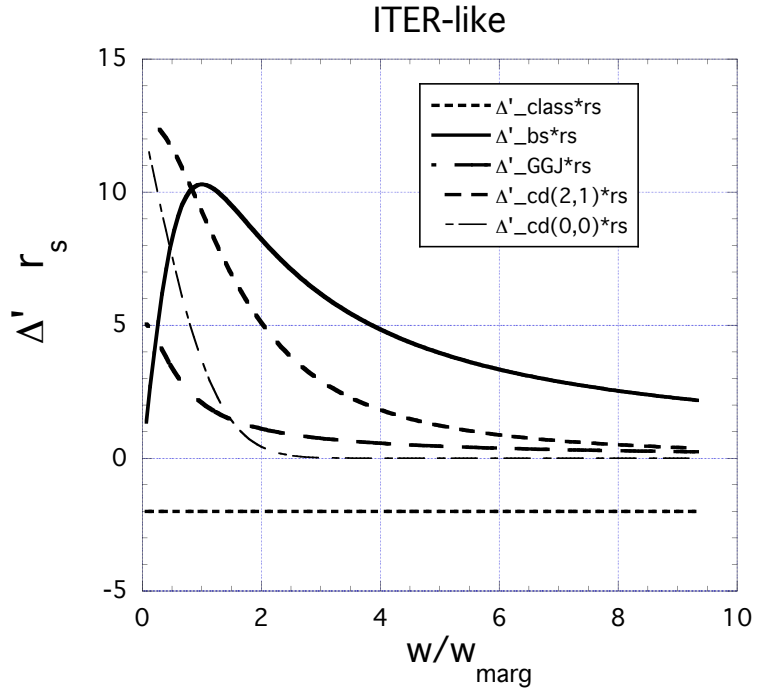

FIG. 2. *Contributions to neoclassical* Δ' *vs* w/w_{marg} *for m=2,n=1 NTMs in ITER-like scenarios. Classical* Δ'_0 *(dotted line); neoclassical (bootstrap-driven, full line)* Δ'_{bs}*; toroidal* Δ'_{GGJ} *(thin-dashed line); helical rf current contribution* $\Delta'_{CD(2,1)}$ *(dashed line);axisymmetric rf current contribution* $\Delta'_{CD(0,0)}$ *(thick dashed line)[12].*

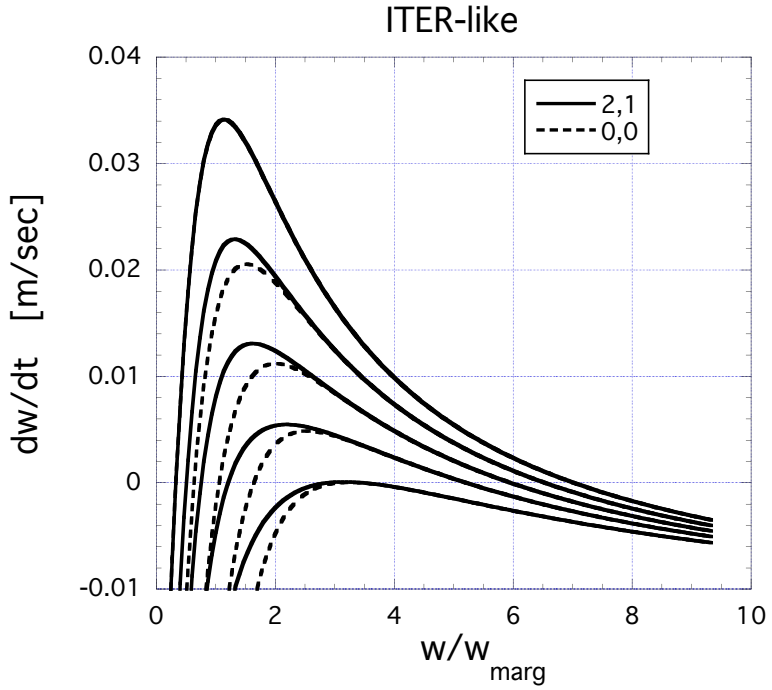

FIG. 3. *NTM phase space dw/dt vs w; example of control of m=2,n=1 NTM magnetic island width down to the self-extinguishing value* w_* *,by perfectly phased* J_{CD} *injection in an ITER-like scenario.*

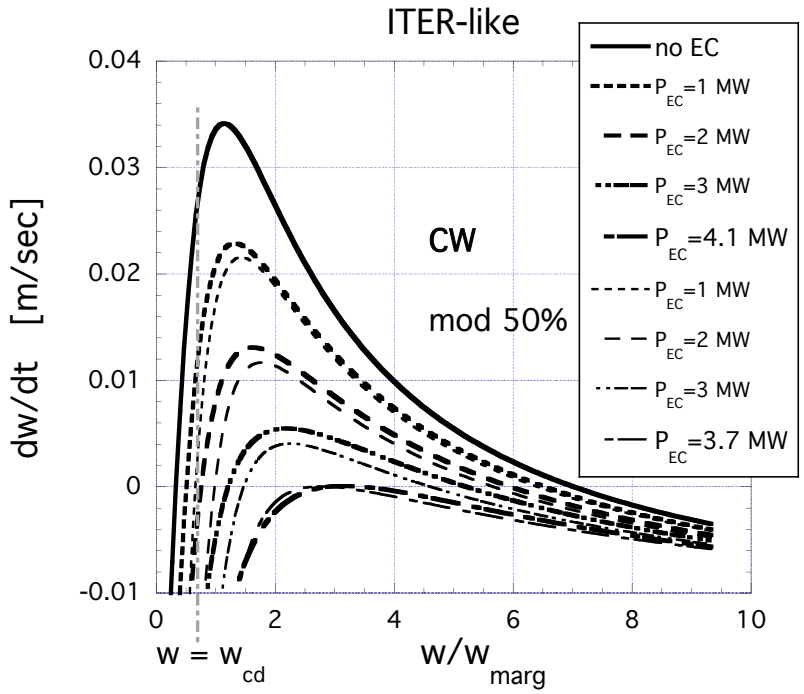

FIG. 4. *NTM phase space dw/dt vs w; example of control of m=2,n=1 NTM magnetic island width down to the self-extinguishing value* w_* *,by perfectly phased* J_{CD} *injection in an ITER-like scenario. showing difference between CW (0*$\leq$ $P_{EC} < 4.1MW$*) and 50% modulated case CW (0*$\leq$ $P_{EC} < 3.7MW$*).*

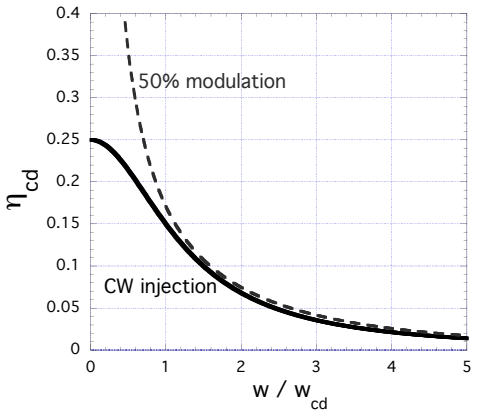

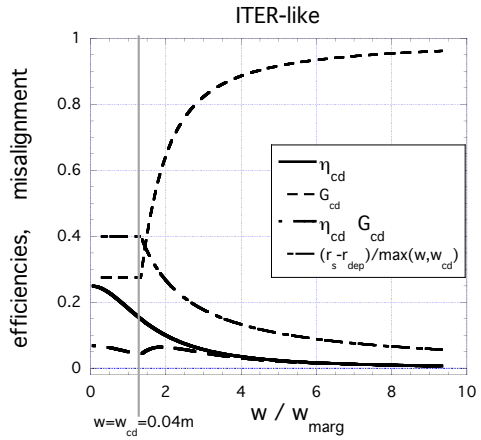

FIG. 5. *(Top) ECCD (helical) efficiency for control of m=2,n=1 magnetic island, with CW or 50% modulation of J_{CD}, perfectly phased and radially aligned on O-point ;(bottom) plots of $\eta_{CDm.n}$ G_{CD} with the effect of radial misalignment δR.*

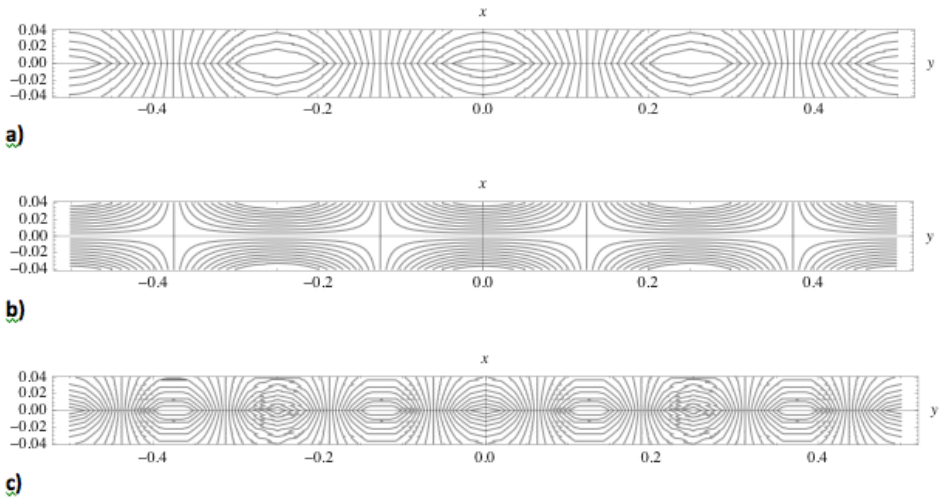

FIG. 6. *Response of HKT ψ_{II} state to J_{CD}(Eq.(22)):a) initial island wth no J_{CD}; b) case of island suppression with $\delta_{CD} \sim w$;c) same as b) but with δ_{CD} reduced by* 20%*: islands and current sheets appear.*

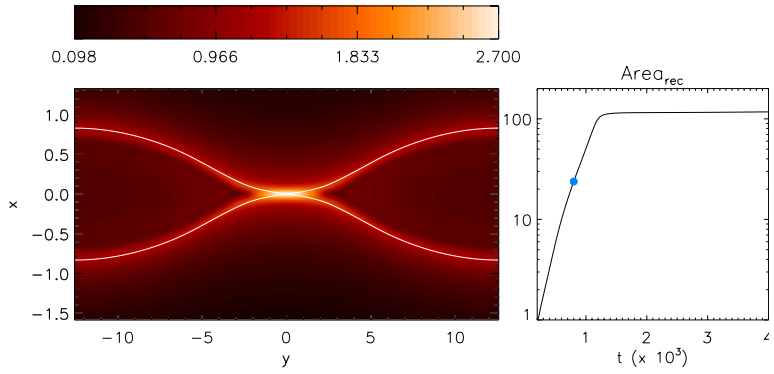

FIG. 7. *Left frame. Contour plots of the current density at the time $t_1 = 800$, when the ECCD starts to be injected. The superimposed white lines identify the borders of the corresponding magnetic island. The rigth frame shows the time evolution of the magnetic island area in absence of ECCD control.*

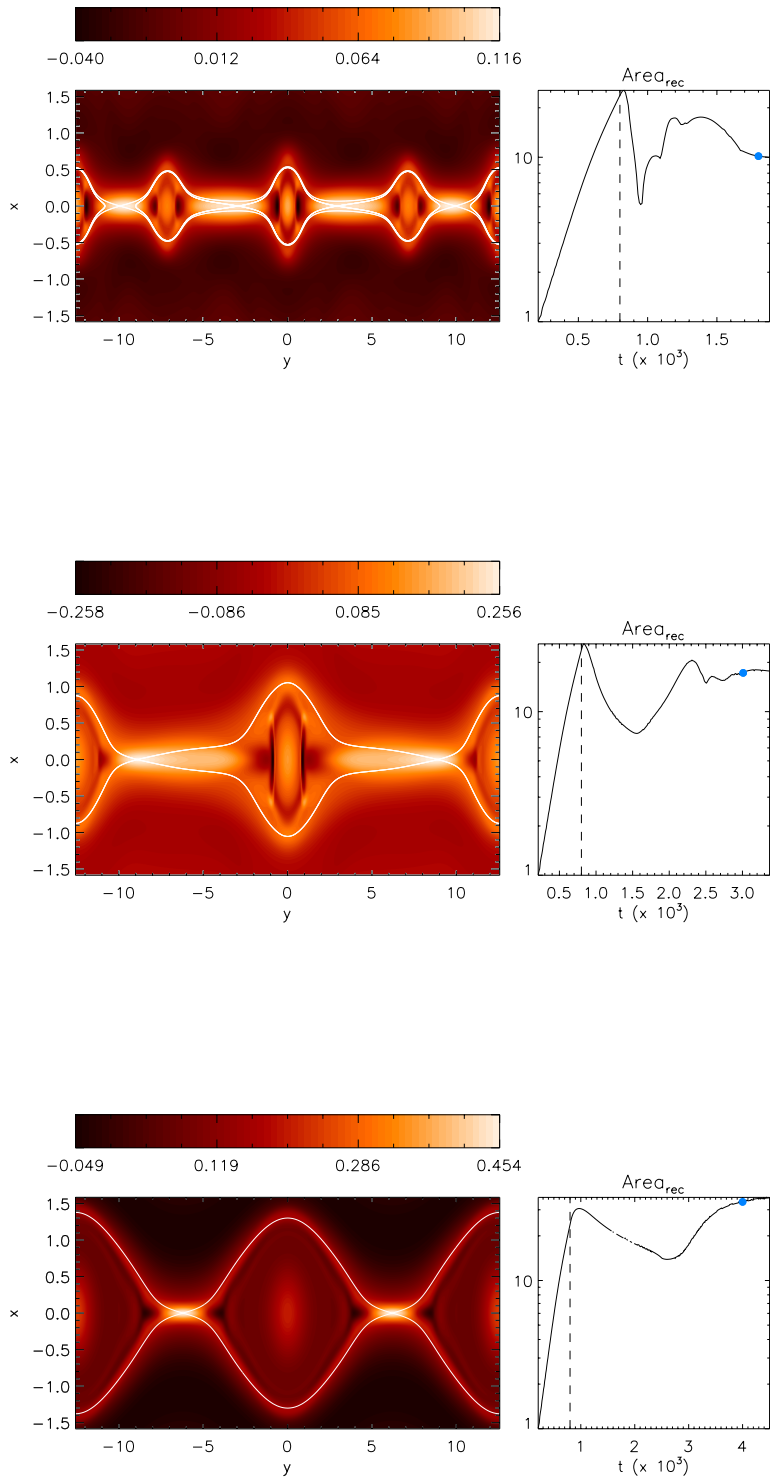

FIG. 8. *Left column, from top to bottom. Contour plots of the current density in presence of ECCD beams of width* $\delta_{CD} = b[\psi_X - \psi_O]$ *with* $b = 0.5, 1, 2$. *The superimposed white lines identify the borders of the corresponding reconnected region. The rigth column shows the time evolution of the area of the reconnected region for the three cases. The dashed lines identify the starting injection time* $t_1 = 800$, *while the blue dots show the time when the current is plotted.*

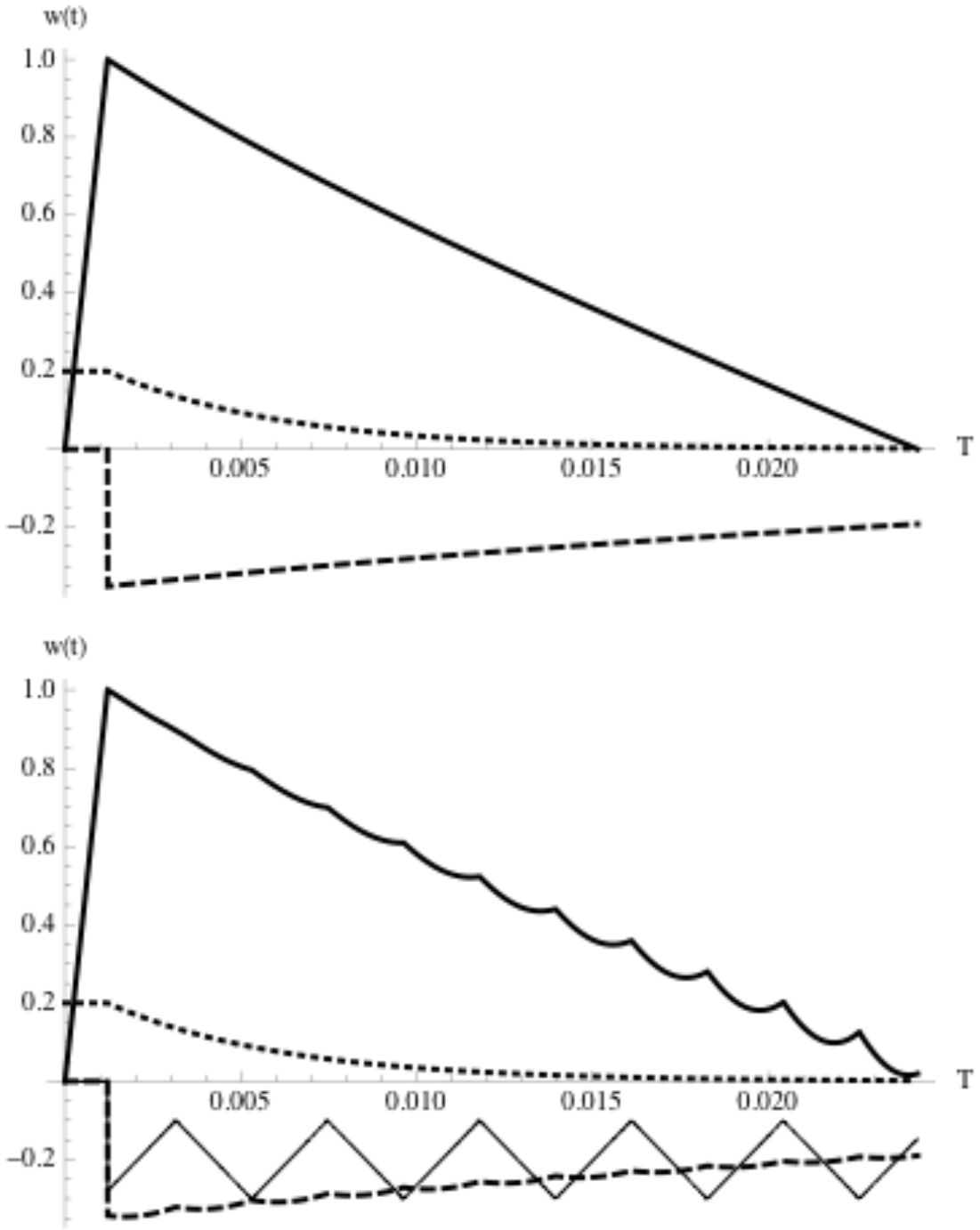

FIG. 9. *Result of Optimal Control. (top)-a) (full line) suppression in minimal time T of the incipient island width (normalzed at start of the control);b) (dotted) evolution of the frequency (normalized);c) (dashed) evolution of the control function U(t) (in a.u.) for fixed ,small, radial misalignment); (bottom)-Result of "Piecewise Optimal Control". a) (full line) Suppression in minimal time T of the island width with intermittent sweeping of rational surface;b) (dotted) evolution of the frequency;c) (thin full line) offset waveform of the radial displacement (t); d) (dashed) evolution of the resulting control function U(t) (in a.u.).*

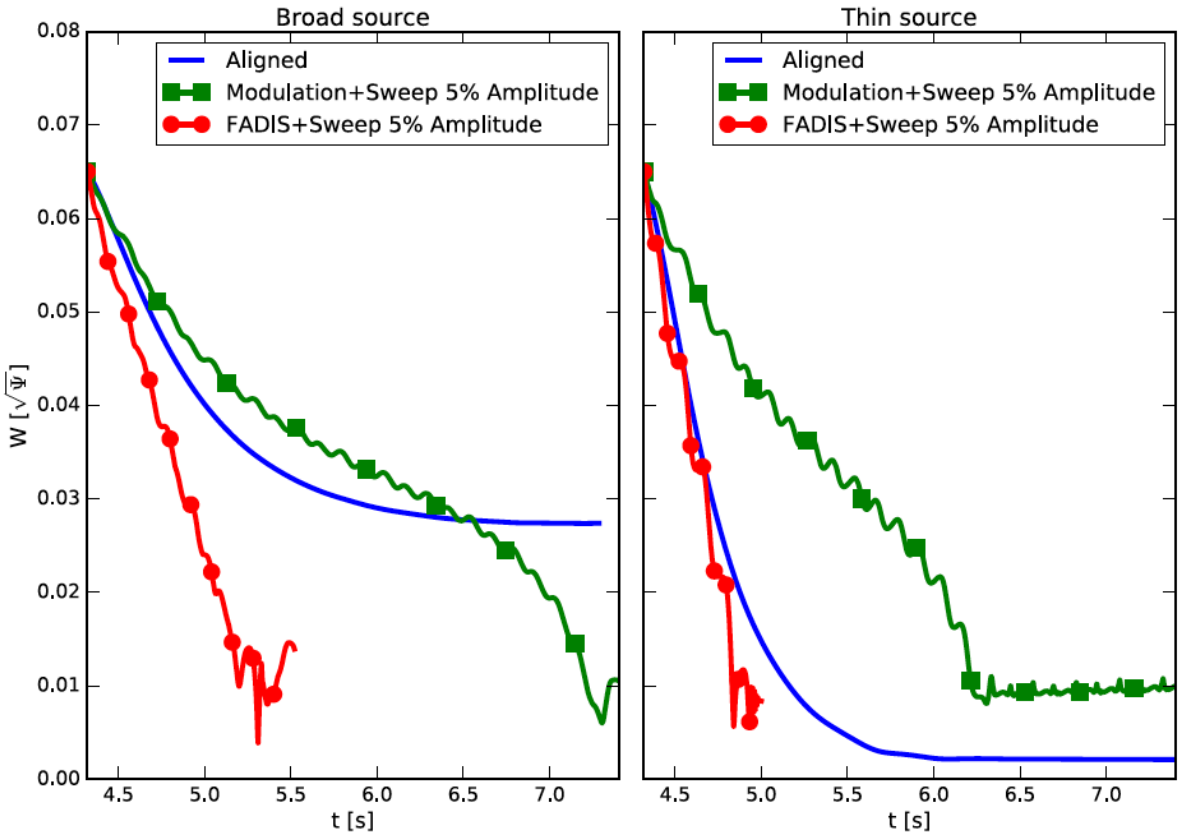

FIG. 10. *Results of XTOR modelling by [50] of island stabilization by combined methods (modulation + rf beam sweeping or FADIS + rf beam sweeping); In both cases, the island can be suppressed or drastically reduced, proving that these schemes are robust towards misalignment or deposition width uncertainties [O.Fevrier, P.Maget, H.Lutjens, P.Beyev,Plasma Physics and Controlled Fusion,59:044002, 2017]*

.

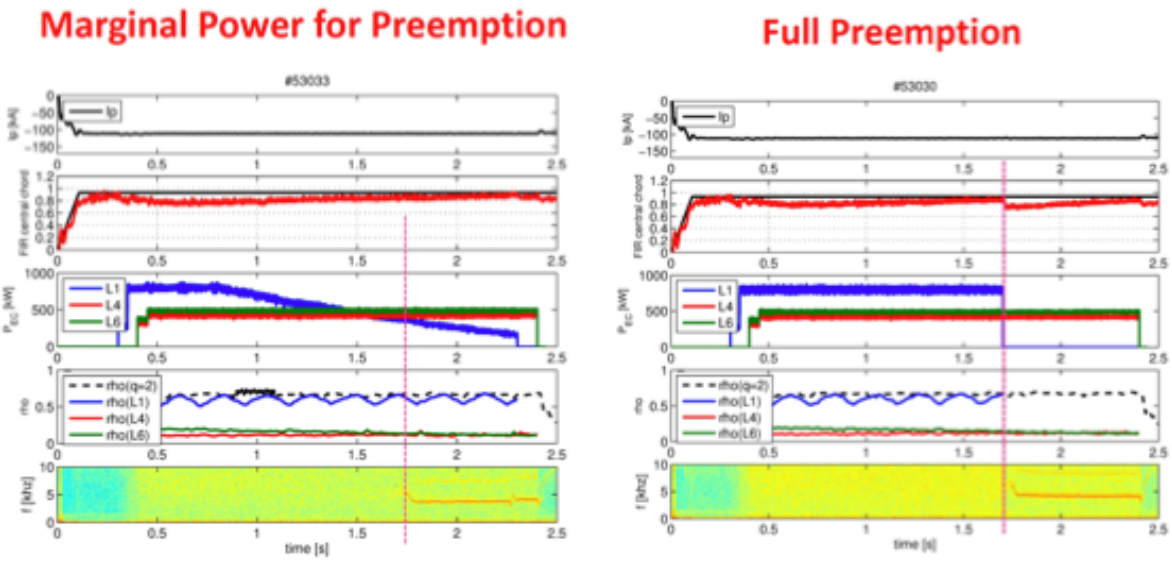

FIG. 11. *Robust NTM control on TCV by intermittent sweeping of q-rational surface.From top to bottom: time traces of plasma current I_p, FIR signal, $P_{EC}(kW)$ of Gyroltrons L_1,L_4, L_6,sweeping waveform of (normalized) deposition radius ρ , spectrogram of modes (khz). In the left frame, the marginal power for pre-emption is found at $t \sim 1.75s$.In the right frame, full stabilization is achieved with P_{EC} larger than marginal value sweeping across the rational-q surface [O. Sauter et al, MST1 (2016)].*

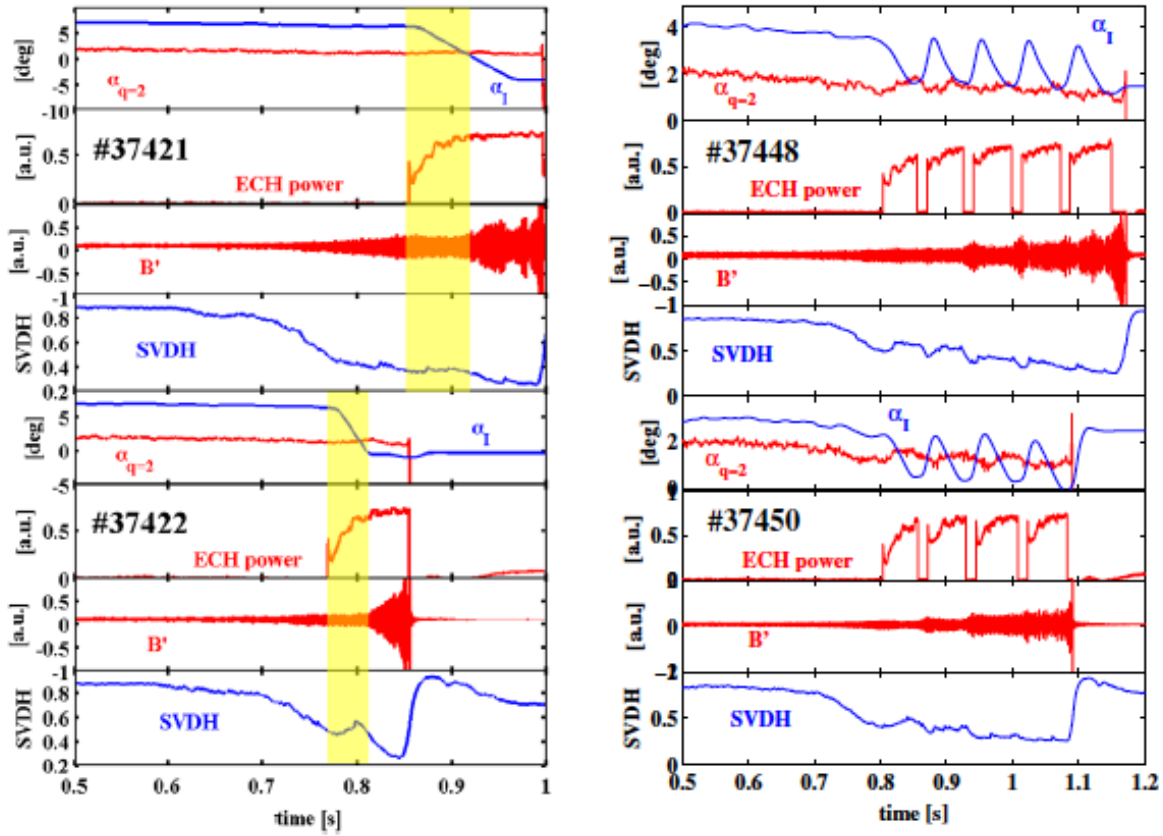

FIG. 12. *Time evolution of the main r-t signals available during the MHD control experiment. A poloidal scan of the ECRH deposition is performed around the 2,1 island region. From top to bottom for each shot: RT reference angles of the poloidal injection of ECRH (0: horizontal, negative: inboard) and of the q = 2 surface; ECRH power (in a.u.); pick-up coil signal (a.u.); SVDH marker. In these pulsed scans the ECRH power is switched off moving outward and switched on moving inward. The MHD oscillations appear depressed by ECRH pulses [C.Sozzi, G. Galperti,E. Alessi, et al,Nucl. Fusion* ***55*** *083010 (2015)].*